1   Towards Grid Friendly Zero Energy Buildings

2

3

4   Philipp Bruggmann [a,*]

5   [a] University of Colorado Boulder

6   Civil, Environmental and Architectural Engineering

7   UCB 428, Boulder, CO 80309-0428

8   USA

9   philipp.bruggmann@colorado.edu

10   * Corresponding Author

11

12   Gregor P. Henze [a]

13   [a] University of Colorado Boulder

14   Civil, Environmental and Architectural Engineering

15   UCB 428, Boulder, CO 80309-0428

16   USA

17   gregor.henze@colorado.edu

18

19   Total number of words used: 5172

20

21

Abstract

High performance buildings such as zero energy buildings (ZEB) are an important step towards a reduction in greenhouse gas emissions. Since ZEB may exhibit large differences between demand and onsite generated electricity, residual electrical loads imposed by the building may fluctuate between positive and negative values. Furthermore, such buildings can be characterized by large temporal changes in residual load, commonly caused by clouds passing on a sunny day. Today, electricity grid operators can easily deal with a single ZEB with this behavior. But what happens if large portfolios of ZEB have the same behavior? In this study, a highly efficient office building with a total floor area of 8'355m^2 located in Denver, Colorado was designed and simulated using a detailed building energy modeling approach. Combining the building energy model with a photovoltaic model showed that the building reached net positive status on an annual basis. Further analysis of residual loads as well as strategies for their reduction revealed the limited potential due to the comparatively high shares from interior lighting and equipment in the energy use distribution. Using a multiple objective optimization approach for optimizing several simplified electric and thermal storage systems allowed comparing different strategies for residual load reduction. Although electrical storage may not yet be economical given today's system costs, it could be shown that the residual loads can be effectively managed and reduced, while at the same time, an increase in photovoltaic self-consumption can be achieved. The analysis concludes with the presentation of a multi-objective optimal solution (Pareto front) for a battery storage model, indicating what utility incentives would be required to achieve cost effectiveness for a range of battery system price scenarios.

Keywords

1. Introduction

1.1 Motivation

The building sector in the U.S. consumes approximately 41% of the nation's total primary energy use. Additionally, the building sector is by far the largest consumer of electricity, representing 74% of annual electricity sales. Considering that 66% of the total electricity production is coming from fossil fuels, makes the greenhouse gas footprint of buildings even worse (U.S. Department of Energy 2015). Undoubtedly, there is a wide range of improvement opportunities. One of them are zero energy buildings: Using highly efficient appliances, daylight optimized designs, high performance envelopes and windows reduces their energy consumption to a minimum, while on-site energy production systems decrease the annual energy consumption to zero or even into positive territory. Aside from all advantages there is one major drawback: high residual loads (RL). Electricity grid operators who provide and maintain the electrical grid do not gain a profit at the end of the year, and even worse, they must ensure grid stability which is jeopardized by the highly volatile residual loads of zero energy buildings. Extensive literature about the design of zero energy buildings is available (Hall 2014; Athienitis, O'Brien 2015; Kolokotsa et al. 2011; Judex 2012). The UW Building Energy Research Group (BERG) for example has over thirty publications about zero energy buildings and related topics (UW Berg). Furthermore, there are numerous studies ongoing investigating the influences and risks of feed-in electricity from onsite PV generation as well as distributed and centralized energy storage strategies aimed at maintaining grid stability (Milo et al. 2011). To the authors' knowledge, no prior work combined these topics and elaborated a whole building simulation modeling approach in terms of grid friendliness.

1.2   Problem Statement

High performance buildings such as ZEB are a step towards a reduction in greenhouse gas emissions.

Nonetheless, one of their major drawbacks as mentioned above needs deeper examination. Fig. 1

shows the uncontrolled residual load profile over one day of the Research Support Facility at the

National Renewable Energy Laboratory in Golden, Colorado (Shanti Pless). A peak residual load

difference of about 2 MW can be seen at this specific day. Even worse, there are also significant high

ramping events in the morning, probably due to clouds, and in the evening when the sun sets.
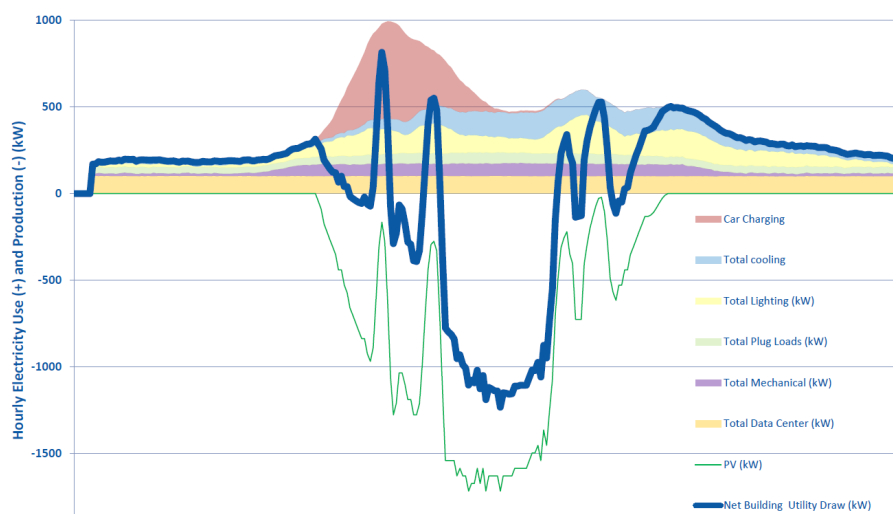
Fig. 1. Uncontrolled Load Profile for a Zero Energy Building NREL RSF

1.3   Objectives

The first objective was an identification of optimal design approaches for a zero energy building.

Hence, different building shapes, envelope alternatives, insulation types, orientations and other

variations have been considered for possible improvements. The second objective was an analysis of

the dynamic residual electrical loads and appropriate strategies for their mitigation and reduction.

1.4   Zero Energy Building Definition

This work adopts the current official definition of a zero energy building authored by the Department

of Energy (DOE): "An energy-efficient building where, on a source energy basis, the actual annual

delivered energy is less than or equal to the on-site renewable exported energy." (U.S. Department

of Energy).

1.5 Residual Load Definition

While the term residual load may have different interpretations, throughout this study the term

residual load is defined as the difference between electricity demand and the on-site electricity

production; positive residual loads imply demand from the grid and negative residual loads feed-in

electricity to the grid.

2. Methods

To achieve the objectives of this study, it was necessary to focus on several different characteristics of zero energy buildings. Building geometry, orientation, envelope types, fenestration, heating, ventilation and air conditioning (HVAC) systems, and on-site renewable energy systems are just a few among them. Since this study will serve as a foundation for future studies and many aspects of building design had to be considered, a simulation approach was chosen. Because OpenStudio provides an easy-to-use building simulation environment and additionally is open source it was used as modeling software. To compare different concepts, the Parametric Analysis Tool (PAT) also provided by the National Renewable Energy Laboratory (NREL) was adopted. Since OpenStudio does not yet allow implementing advanced HVAC system controls, the Energy Management System (EMS) for EnergyPlus was used. The photovoltaic model for the on-site renewable energy production was developed in the System Adviser Model (SAM) software provided by NREL. It is open source and has a large library with photovoltaic panels and inverter specifications from various manufacturers. Once the building and the photovoltaic model was established, the residual loads were assessed. OpenStudio and EnergyPlus building models provide high accuracy modeling due to the heat balance method for the coupled thermal zones, (U.S. Department of Energy et al. 2015; Zhu et al. 2012). However, since a multiple objective optimization approach was chosen for the residual load reduction strategies and the building simulation required considerable processing power, reduced order models for the heat pump and the storage systems were developed in the technical computing environment MATLAB.

The climate where a building is located has a dominant impact on the design and the U.S. has been divided into eight primary climate zones (ASHRAE 2010). Each climate zone is grouped by the number of heating and cooling degree days (HDD65 and CDD50). These climate zones are further subdivided by three moisture levels, humid (A), dry (B) and marine (C). For each climate zone, different provisions in the salient standards and codes are enforced. Climate zone 5B is valid for Denver where the proposed building is located (ASHRAE 2014a). Proper weather data is crucial for building energy simulation. Fortunately, NREL provides a free library with typical meteorological year (TMY) weather data for simulation purposes, which can be found in the National Solar Radiation Data Base (NSRDB)

127   archive (NSRDB). It has to be noted that TMY data is not suitable for analyzing worst-case scenarios

128   with extreme weather conditions (NSRDB). In the beginning of the design process, TMY data from the

129   Denver International Airport was used for simulations. As the design process evolved, data at higher

130   temporal resolution as described further below had to be used. The dynamic behavior of the electricity

131   production from the photovoltaic (PV) system is important for subsequent residual load analysis; thus,

132   a higher resolution weather data was therefore needed. Since one-minute based data was only

133   available for the location in Golden, Colorado, the solar radiation, temperature and humidity values

134   for Golden were used in the context building simulation. For the remaining values, TMY data from the

135   Denver International Airport were used.

136

# 3. Simulation Model Development

3.1 OpenStudio Building Model

3.1.1 Building Envelope

The surface-area-to-volume-ratio is an important factor affecting the energy needs of a building. A large surface area leads to a significant energy exchange between the envelope and the environment. Hence, the higher the area-to-volume (A/V) ratio, the higher the energy needs should be. Considering a floor height of 3.8 meters and a total floor area of 8'500 m^2, the lowest A/V ratio was evaluated for different number of floors. From 4 to 8 floors, the ratio is about 15%. Reducing the number of floors, leads to an increase in A/V ratio up to approximately 30% for a single-storey building. Since the influence of weather impacts, ground heat exchange and other interactions are not considered by the A/V ratio, a parametric analysis for different number of floors, window-to-wall ratios, aspect ratios and orientations has been conducted. The simulation for this analysis were highly simplified. The option "Ideal Air Loads" was used in OpenStudio (NREL 2015), therefore neither a ventilation nor a heating and cooling system had to be designed. In this case, EnergyPlus assumes perfectly met comfort conditions. For the sake of simplicity, no shading and daylight control were considered. Analyzing the results from the Parametric Analysis Tool (PAT) revealed a surprising outcome. The single-storey building has the lowest combined cooling and heating demand. Since this result, due to the high A/V ratio, was not expected, a reason for this behavior had to be found. Changing the ground surface conditions as adiabatic, effected the expected behavior; a taller building has lower cooling and heating demand than a single-storey building. Thus, the reason for the unexpected results is the strong impact of the ground heat exchange. Constant ground temperatures from the EnergyPlus Weather (.epw) data Denver International Airport were used (U.S. Department of Energy et al.). Considering the land price in Denver and the use of daylight, further simulations adopted a three-storey building.

161   3.1.2   Window-to-Wall Ratio

162   The optimal window-to-wall (W/W) ratio is challenging to choose but essential for a zero energy

163   building. An optimum between heating and cooling losses, daylight savings and solar gains must be

164   found. Fig. 2 shows the energy needs depending on the W/W ratio. The dashed line illustrates the total

165   source energy needs without windows whereas the dotted line shows a baseline case with 40% W/W

166   ratio and American Society of Heating, Refrigerating and Air-Conditioning Engineers (ASHRAE) 90.1-

167   2004 window specifications (U-factor 3.12 W/m^2, SHGC 0.4, VLT 0.31), but without daylight control.

168   The total source energies are on the primary y-axis whereas the energy use of the interior lighting,

169   district heating and cooling are on the secondary y-axis. As expected, the total source energy needs

170   are a lot lower with triple pane windows. Due to the large savings, the designed building was finally

171   equipped with triple pane windows. Regarding Fig. 2, the total source energy needs are lowest at 20%

172   W/W ratio (U-factor 0.785 W/m2, SHGC 0.474, VLT 0.661). Therefore, approximately this ratio was

173   adopted in the proposed building design. The fact that daylight also has an important role considering

174   employees comfort, would justify percentages higher than the energy optimum.
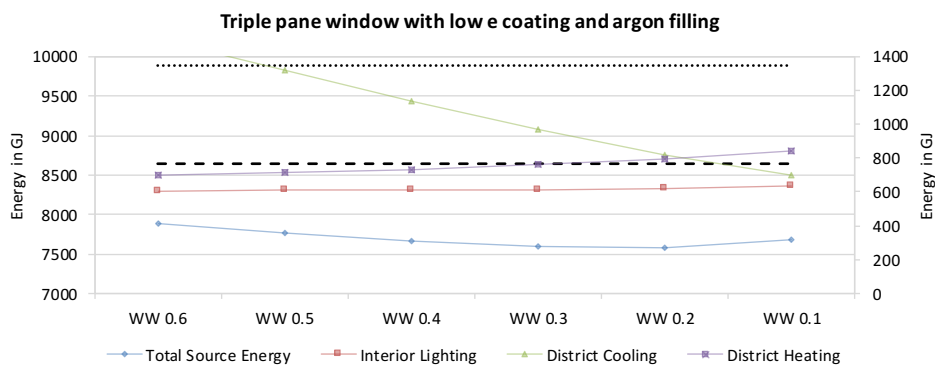
Fig. 2. Evaluation of the Window to Wall Ratio

3.1.3 Aspect Ratio

The aspect ratio (ratio of building length to width) was varied from 1.0 (square) up to 3.0. Since the cooling and heating energy demand did not change significantly but daylight penetration at the preferred south and north façade is favored with higher ratios, a ratio of 2.0 was chosen. The orientation (0° represents a southern orientation) of the building was changed from 0° up to 60°. Since south-north orientated buildings have better daylight penetration and east and west facing surfaces are hard to shade effectively, a south orientation was considered in the designed building. Square and rectangular shapes have less dead space and are cheaper to build compared to other shapes. On the other hand, wind optimized shapes could have a beneficial impact on the total energy use . Since Denver does not have constant high wind velocities, the building was designed in a rectangular shape using the aspect ratio of 2.0. Because Denver features an almost optimal climate for natural ventilation (dry and low temperatures during the night), an atrium was included in the center of the building.

3.1.4 Floor Plan

Following the analyses described in the sections given above, the floor plan could be sketched using common space program assumptions shown in Table 1 (ASHRAE 2014b). In category Others, a printing room as well as an information technology (IT) room were considered. The total needed ground area is 2'850 m^2.

3.1.5 Roof Type

Pitched roofs come in a variety of styles, such as gable, cross gable and hipped, all sloped to different degrees. Their installation cost is usually higher than a flat roof, but since flat roofs need more maintenance regarding the sealing, the long-term costs are similar. Another important point to mention is the dead volume. Office buildings usually do not have an attic. Hence, the lost volume related to the pitched roof cannot be used as effectively as in residential buildings. Since a photovoltaic system is very likely on a ZEB and pitched roofs are less flexible concerning later orientation changes, a flat roof was considered for the designed building model.
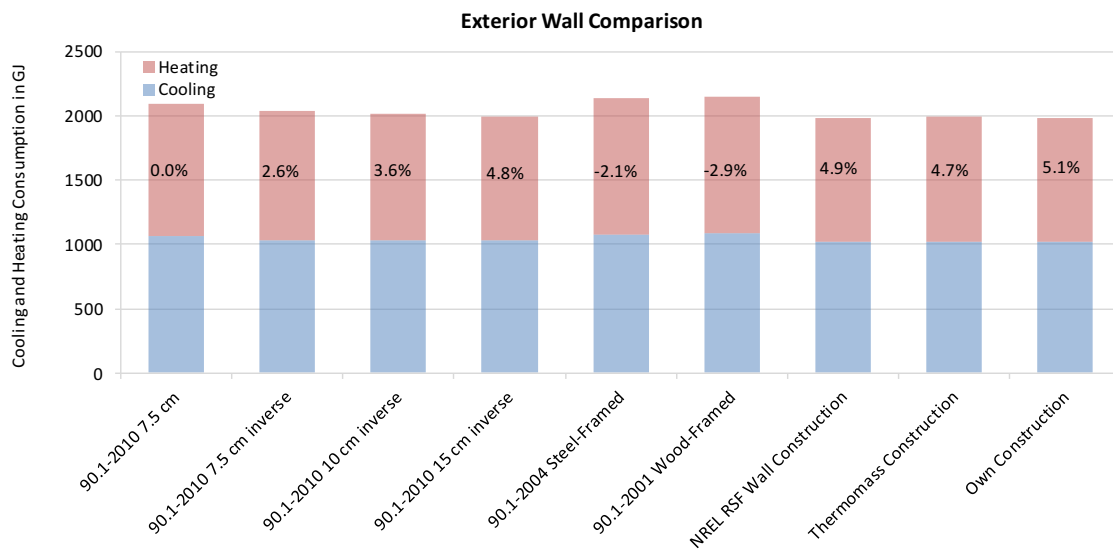

3.1.6 Wall Construction

To reach the goal of a zero energy building, the energy demand should be as low as possible but the building should still be affordable. Exterior walls including their insulation play an important role in this case. To evaluate the exterior walls, different wall types and insulation thicknesses were compared, shown in Fig. 3. The first construction uses the OpenStudio default recommendations for an exterior mass wall according to ASHRAE 90.1-2010 (ASHRAE 2010). This construction consists of an interior insulation and a concrete mass wall. Since exterior insulations have different benefits such as reduced condensation problems and the use of thermal mass, the construction layers were switched. Just by doing so, the combined heating and cooling needs could be reduced by 2.6%. Increasing the insulation thickness effected a decrease in cooling and heating energy as well. The two other construction types, as well OpenStudio default recommendations, a steel-framed and a wood-framed wall increased the energy demand. In order to make a decision on the insulation thickness, different studies on economical insulation thickness optima were reviewed (Jozsef Nyers, Slavica Tomic, Arpad Nyers 2014; Çomaklı, Yüksel 2003; Martin Jakob 2004; Nematchoua et al. 2015). Summarizing the literature, an insulation layer of about 10 cm is considered the optimum economical thickness. One study showed that if longer payback times were permitted, thicker layers are favored (Martin Jakob 2004). Thermal mass is another important factor for an exterior wall construction. The higher it is, the more thermal

223 storage capacity is available and this in turn increases comfort, due to slower changing zone

224 temperatures. Furthermore, it allows shifting the supplied cooling and heating to economically

225 favorable hours. These considerations lead to three additional wall constructions. Thanks to the

226 assistance received from a wall construction company, the wall construction previously used in the

227 Research Support Facility building on the campus of the National Renewable Energy Laboratory could

228 be modeled (U.S. Department of Energy). Moreover, they suggested a construction set located in

229 Denver. Considering thermal mass and insulation, a custom assembled construction was introduced as

230 well.

231

232

233 *Fig. 3. Exterior Wall Performance Comparison including their U-Value*

234 The wall construction company provided one overall R-Value which also considers wall connectors.

235 Since OpenStudio requests values for each layer, they were evaluated using literature for the material

236 properties (Fundamentals 1997). Comparing the evaluated with the provided R-Value showed an error

237 of about 3%, which was assumed to be sufficiently accurate. Fig. 4 shows the selected wall construction
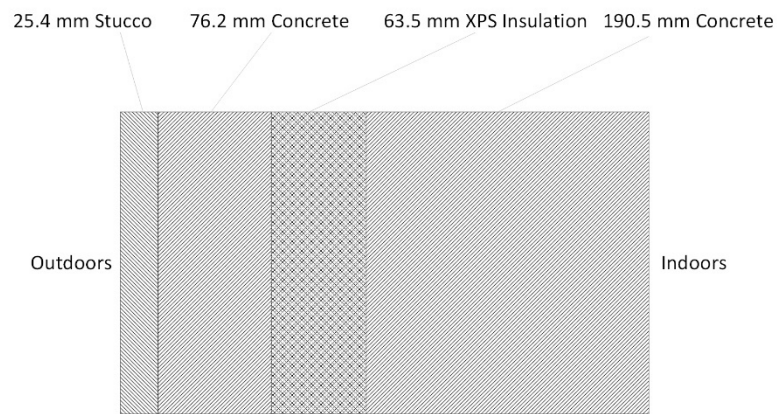
238 suggest by Thermomass.

239

25.4 mm Stucco   76.2 mm Concrete   63.5 mm XPS Insulation   190.5 mm Concrete

Outdoors

Indoors

240

241

Fig. 4. Suggested Wall Construction

242   The exterior roof was selected following the Advanced Energy Design Guide from ASHRAE that

243   recommends an R-Value greater than 4.56 m^2K/W for climate zone 5 (ASHRAE 2014b). A pre-

244   assembled construction from the building component library (BCL) with a matching R-value was

245   adopted in the building model (Building Component Library). The construction consists of three layers:

246   a metal decking, an insulation layer with a thickness of 26 cm and a roof membrane.

247   3.1.7   Thermally Activated Building Systems (TABS) Floor Construction

248   OpenStudio uses internal source constructions to model radiant floor and ceiling systems. Therefore,

249   each surface which is part of the radiant cooling or heating system needs to be assigned to this

250   construction set. The different construction layers must be manually specified in OpenStudio.

251   Furthermore, the location of the hydronic piping and the temperature sensor must be assigned to the

252   desired layer. The implemented internal source construction sets are shown in Fig. 5 and Fig. 6. Using

253   an application handbook and a TABS control guide developed by a building automation manufacturer

254   lead to the selected interior floor thickness of 203 mm (Siemens; Faktor Verlag AG - Architektur,

255   Technik. Energie. Informationen zur Nachhaltigkeit am Bau - TABS-Tool). The piping as well as the

256   temperature sensor were located in the center. No insulation layer was added to the interior

257   construction set. The construction facing the ground consists of a 102 mm concrete layer followed by

258   a 25 mm insulation layer and another 102 mm concrete layer. Thermally activated building systems

259   (TABS) are typically operated at low hot water and high chilled water supply temperatures. Since heat

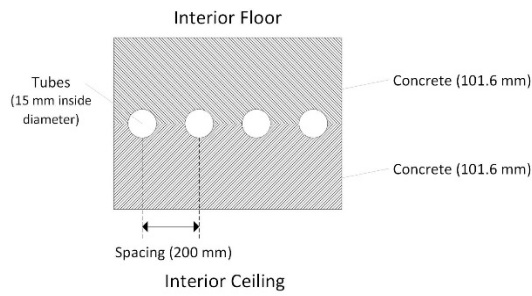260   pumps are more efficient in this context, the decision was made to use this system.
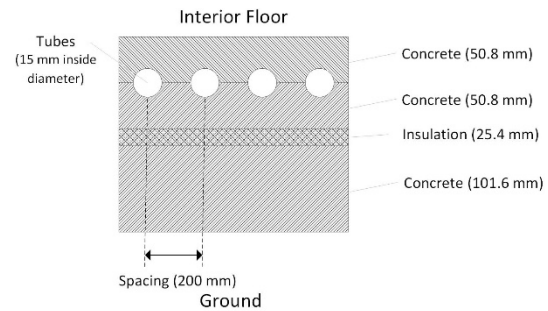
Fig. 5. Internal Source Construction (interior)   Fig. 6. Internal Source Construction (exterior)

261

3.1.8 Daylight Analysis

262

Energy use for electrical lighting represent a significant share of the total energy consumption of a

building. At the same time, it is known that daylight has an important impact to human health and can

increase productivity significantly. The fact that north and south facing offices provide the best daylight

conditions was already considered by selecting an appropriate building aspect ratio. OpenStudio has a

dedicated tool for daylight analysis: The daylight analysis tool Radiance is based on raytracing and has

recently been integrated with OpenStudio (Rob Guglielmetti). The downside of the accuracy of

raytracing are its high computational requirements, making it currently impossible to simulate the

entire building at once. Hence, several representative zones had to be selected and simulated

separately. At least one zone per orientation must be selected to get a robust analysis of daylight

availability. Obviously, the more zones are simulated the more accurate the total savings estimates

are. Simulations showed that interior zones are not affected significantly if interior windows are

applied and both zones (exterior and interior) are simulated together. This outcome reduced the

simulation effort significantly. Radiance provides three different daylight metrics. Daylight autonomy

(DA), continuous daylight autonomy (cDA) and useful daylight illuminance (UDI). By using eight

representative zones it was possible to compare several different measures to increase and optimize

daylight savings. Based on the more accurate evaluation algorithm of Radiance those results are more

accurate than the radiosity (split flux) based approach that OpenStudio uses in the EnergyPlus engine.

280 As mentioned above, the annual electrical lighting distribution of the entire building could not be

281 evaluated by the Radiance approach. Therefore, the best options evaluated with the Radiance

282 approach were applied to the whole building model and simulated again. Table 2 shows the tests

283 options for daylight optimization for which the illuminance set point was set at 500 lux. Fig. 7 shows

284 the site energy savings with total annual savings of 10%. The difference between the Radiance and

285 radiosity based approaches was smaller than 1%, so the inaccuracy was deemed acceptable.

286

287

Energy Savings due to Daylight Control
without Radiance
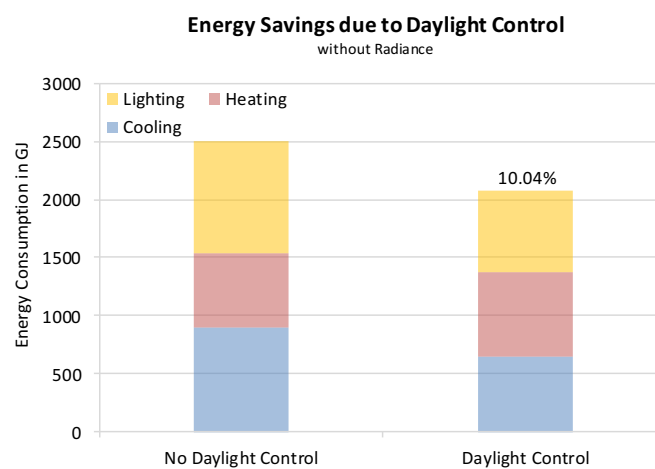
Fig. 7. Energy Savings due to Daylight Control

288

289

290 3.1.9 Final Building Design

291 The findings described in Sections 3.1.1 to 3.1.7 resulted iteratively to the three-dimensional building

292 model. Fig. 8 shows the final building model with the entrance on the east side. Using the same window

293 and shading objects for the whole building is favorable for cost reasons. In total, 6'638 m^2 are

294 conditioned and 1'718 m^2 are unconditioned. The south and north façade have a window-to-wall ratio

295 of 22% whereas the east and west façade have one of 15%.

296

297
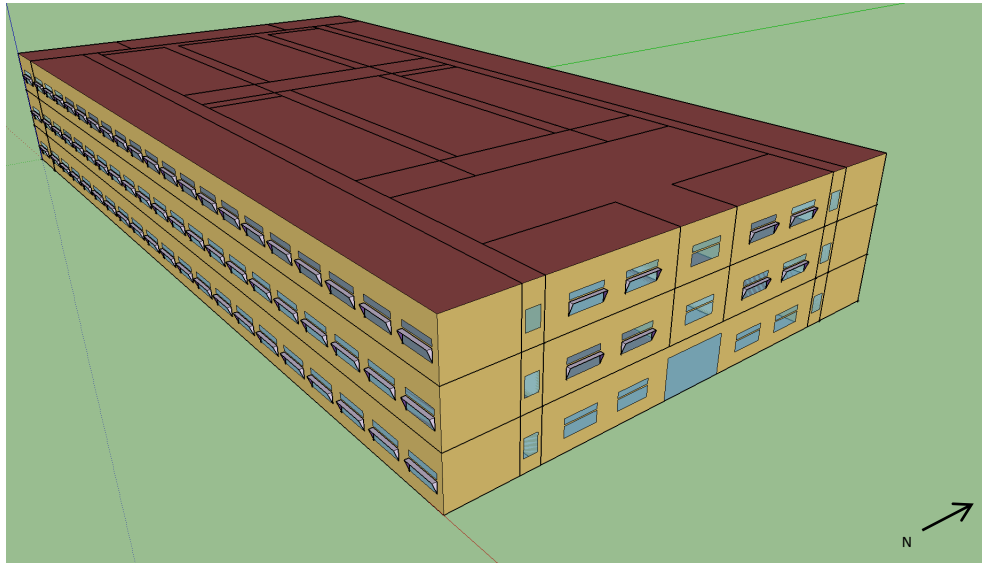
Fig. 8. Final 3-D Building Model

298

299

300

301

302 ### 3.1.10 HVAC System

303 Heating, ventilating and air conditioning (HVAC) systems provide heating, cooling, humidification,

304 dehumidification and air quality control to satisfy the occupant needs. There are two main system

305 options: Central HVAC systems which are, for example used in commercial office buildings and

306 decentralized HVAC systems, such as an individual room air conditioner, as they can be found in motels

307 or smaller office buildings. Even though decentralized HVAC system can be appropriate for very specific

308 applications, higher maintenance costs, construction constraints, noise, and commonly a lower overall

309 efficiency make them second choice for newly constructed buildings. Due to the stated reasons, a

310 decentralized system was not considered in the designed building (U.S. Department of Energy; Henze

311 2016).

312 Due to the low heating and high cooling supply water temperatures, a thermally activated building

313 system (TABS) combined with a heat pump can be one of the most efficient HVAC system

314 configurations available; therefore, a TABS combined with a ground source heat pump was selected

315 for the designed building (Informationsdienst). In order to meet air quality standards, a demand

316 controlled ventilation, dedicated outdoor air system (DOAS) with a heating and cooling heat recovery

317 system was used. It provides the occupied zones with 22°C pre-tempered fresh air. In addition to the

318 DOAS, natural ventilation was implemented for night pre-cooling. Since office buildings have very low

319 service hot water needs, those systems offer a lower potential for energy savings, but nevertheless a

320 heat pump water heater was used. Fig. 9 shows a simplified schematic of the modeled HVAC system.

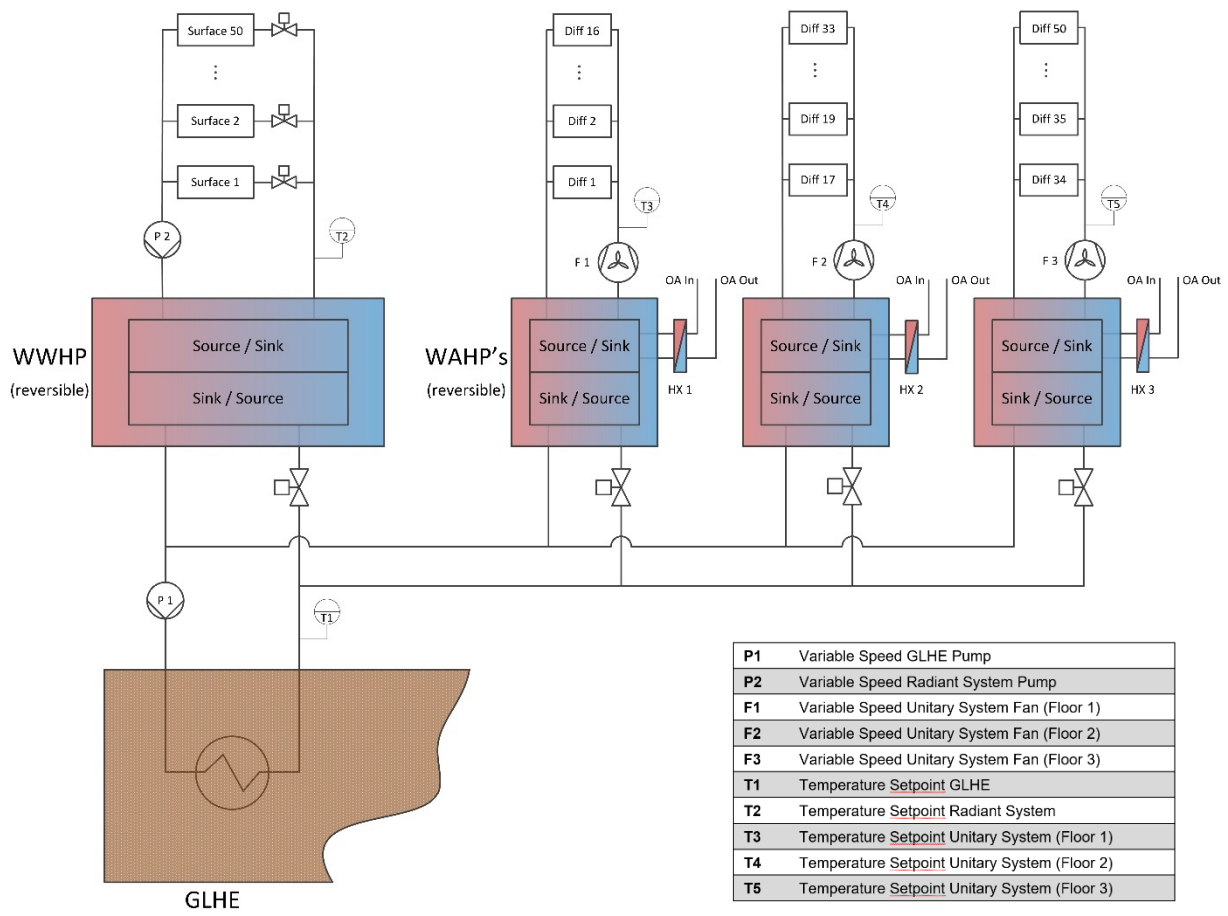321 The key performance metrics of the proposed building are described in Chapter 4.

Fig. 9. HVAC Schematic

P1	Variable Speed GLHE Pump
P2	Variable Speed Radiant System Pump
F1	Variable Speed Unitary System Fan (Floor 1)
F2	Variable Speed Unitary System Fan (Floor 2)
F3	Variable Speed Unitary System Fan (Floor 3)
T1	Temperature Setpoint GLHE
T2	Temperature Setpoint Radiant System
T3	Temperature Setpoint Unitary System (Floor 1)
T4	Temperature Setpoint Unitary System (Floor 2)
T5	Temperature Setpoint Unitary System (Floor 3)

3.2   On-Site Renewable Energy

ZEB's, as described in Section 1.5, have to have a zero or a negative source energy balance on an annual base, requiring on-site renewable energy generation such as solar or wind power. In this study, only a photovoltaic system was considered. The PV system was modeled with the System Advisor Model Software (SAM) (System Advisor Model 2016). It is capable of simulating various types of on-site energy production plants but for this project only the photovoltaic tool was used. Since hundreds of PV panel and inverter specifications from several suppliers are preloaded, it is a lot easier to model the system. SAM allows the user to set the numbers of strings and rows manually. By selecting the orientation and the ground coverage ratio, SAM considers self-shading losses. Furthermore, it was possible to consider the adjacent buildings as shading objects. Selecting soiling and balance-of-system losses completes the technical design of the system. The effects of dynamic weather changes on the electricity production is crucial for residual load analysis, therefore weather data at higher temporal resolution had to be used for the simulation. Fortunately, minute-by-minute data was available from the solar radiation research laboratory (BMS) at NREL (Stoffel, Andreas 1981). The photovoltaic array was designed in an iterative approach by comparing the total on-site electricity production and the annual electricity demand. It turned out that the annual production of the roof array was not high enough to achieve ZEB status. Therefore, the south, east and the west façades were also considered as solar collection area. Since the vertically mounted façade panels have a lower efficiency, cheaper thin film panels were considered there. On the roof, 612 PV panels with an installed capacity of 200 kW and on all three facades combined 954 thin film PV panels with an installed capacity of 112 kW were considered. The characteristics of the PV system are shown in Table 3. The differences of the energy production from the east and west façade are explained due to shading from surrounding buildings.

## 3.3 Reduced Order Model for Controls Analysis

3.3.1 Controls

Fig. 10 shows a schematic of the reduced order model developed for the residual load reduction. The residual loads were used as input signal whereas the heating and cooling demand, the reduction of ramping, the additional energy losses and the incremental costs are use as output signals. Inside the model, the heat pump (HP), the hot and cold water storage systems (HWS & CWS) as well as the battery are illustrated. The applied control strategies for the storage systems and heat pump only consider current and past data, i.e., involve no prediction. Thus, the residual load at each time step was used as the input signal. As soon as the residual load becomes negative, the state-of-charge (SOC) of the HWS, CWS and the battery was checked, and depending on their state-of-charge (SOC), charging, discharging or a dormant state of that was selected. For the thermal storage system, an SOC from 0 to 1 and for the battery an SOC from 0.2 to 0.85 was considered. The battery is, because it can be charged and discharged independently from the heating and cooling demand, is more flexible than the thermal energy storage; therefore the HWS and CWS control was prioritized. The thermal storage systems were discharged depending on the heating and cooling demand. As soon as their SOC fell below 10%, the heat pump was turned on and tracked the demand power. This control ensured that the comfort level was never jeopardized. The battery was discharged if the SOC was in between the mentioned range and the residual load was above zero.

3.3.2 Model

The heat pump was modeled as having a constant coefficient-of-performance (COP). Thus, the input electrical power multiplied by the rated COP leads to the heating, respectively, cooling delivered. Neither a start-up time nor a minimum run time was considered. The hot water as well as the chilled water storage was modeled by aggregating the HP's output energy for each time step. A heat transmission loss term is adopted to take heat losses and gains through the storage tank envelope into account. Neither loading nor unloading effects were considered. Because the reduced order model has no interconnection with the thermal building model, heating and cooling demand could not be shifted.

376   The battery was modeled by integrating the power which was transmitted. A charging and discharging

377   rate of 0.5 C was considered. An alternating current to alternating current (AC-AC) as well as an

378   alternating current to direct current (AC-DC) inverter efficiency of 95% was assumed. Even though the

379   constant losses of a battery are low over 24 hours they were also considered. No battery degradation

380   and cycle stability was considered.

381
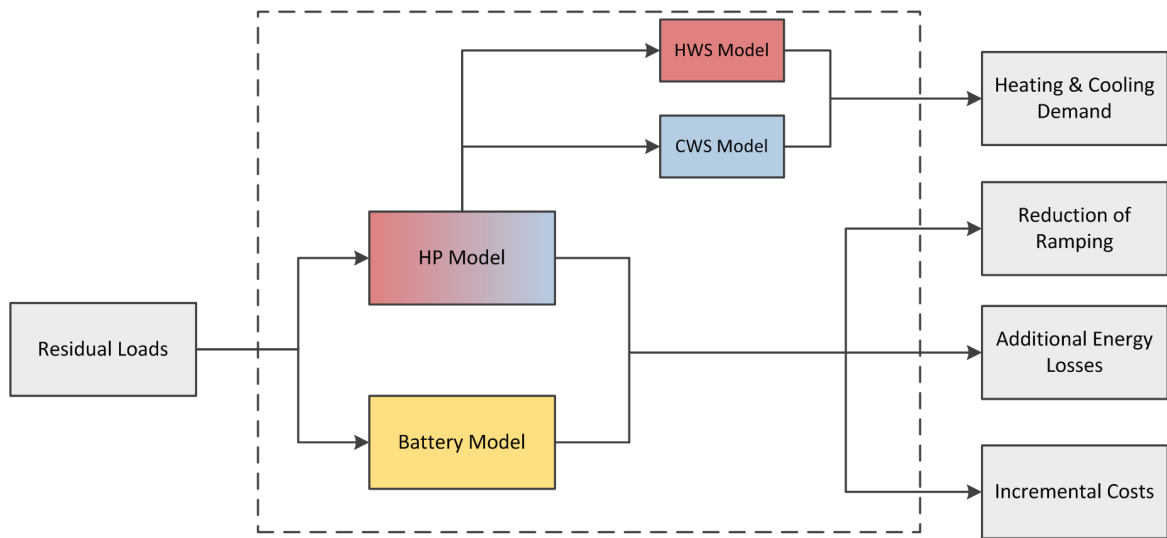
382

383   *Fig. 10. Reduced Order Model for Residual Load Reduction*

384

385 3.3.3 Multiple Objective Optimization

386 A comparison between three different strategies was made to find the most appropriate solution. A

387 thermal storage only, battery only, and a combined configuration were compared. The thermal only

388 storage case could, due to the low heating and cooling demand, not significantly reduce the ramping.

389 To compare the battery only and the combined configuration, a multiple objective optimization was

390 performed. The thermal storage size and the battery capacities were used as decision variables (5).

391 The ramping ratio, which is used for quantifying the fluctuations of the residual load time series,

392 incremental investment costs and the energy losses were selected as objective functions (2) - (4).

393 The optimization problem is defined as in (1).

394

$$\min_{x \in X}\big(f_1(x), f_2(x), f_3(x)\big) \tag{1}$$

$$f_1(x) = \left(\frac{\sum_k^n |P_k^*(x) - P_{k-1}^*(x)|}{\sum_k^n |P_k - P_{k-1}|} \right) \tag{2}$$

$$f_2(x) = \big(C_{Therm} x(1) x(1)^{-0.3464} + C_{Therm} x(2) x(2)^{-0.3464} + C_{Batt} x(3) x(3)^{-0.1}\big) \tag{3}$$

$$f_3(x) = \Big(E_{Therm,Loss}\big(x(1)\big) + E_{Therm,Loss}\big(x(2)\big) + E_{Batt,Loss}\big(x(3)\big)\Big) \tag{4}$$

$$x = [V_{Cool}, V_{Hot}, C_{Batt}]^T, \quad \begin{cases} V_{Cool} \in [0,100] \\ V_{Hot} \in [0,100] \\ C_{Batt} \in [0, 2500] \end{cases} \tag{5}$$

395

396 $f_1(x)$ is the first objective function where the new ramping is divided by the old ramping; a time step

397 k of 15 minutes was considered for a full year (n). $f_2(x)$ considers the incremental costs of the two

398 thermal and the battery storage. Specific costs of 3'500 \$/m^3 (C_{Therm}) with an exponential scaling term

399 of -0.3464 were selected for the thermal storages (Vogelsanger et al. 2008). The scaling effect

400 represents a nonlinear price trend if the storage size is increased. For the battery, a specific price of

401 1'000 \$/kWh with an exponential scaling term of -0.1 was considered (IRENA 2015). $f_3(x)$ considers

402 the additional energy losses for both the thermal energy and the battery storage systems depending

403 on their storage capacity. Thus, the larger the thermal storage or the battery is selected, the greater

404 the energy losses that will occur. For the thermal energy storage, a specific loss of 10 W/m^2 was

405 selected (AGFW 2015). Losses for the battery were considered with 5%/24 hours (Buchmann 2016). $\boldsymbol{x}$

406 is a vector with the three decision variables including V_{Cool} as the cold water storage volume in cubic

407 meters, V_{Hot} as the hot water storage volume in cubic meters, and C_{Batt} the battery capacity in

408 kilowatt hours.

409

410

411

4. Results and Discussion

4.1 Zero Energy Building Model

Table 4 shows the key performance metrics of the proposed building, while Fig. 11 illustrates the distribution of the annual site energy use. It is remarkable to note that all conditioning systems combined (heating, cooling and fans) only have a share of 17%. This indicates, on one hand, that the designed building is indeed very efficient, on the other hand, it lets one recognize that the potential for residual load reduction through demand side management (DSM) is low. Even though the Advanced Energy Design Guide (AEDG) was used for lighting and equipment, they account for 81 % of the annual energy use. It can be argued, that the used energy needs from the AEDG are still too high for interior lighting and equipment but since the specific energy needs were in a plausible range, no further efforts were mad to reduce this energy needs. Because office buildings have low service hot water use, the low energy consumption was expected.
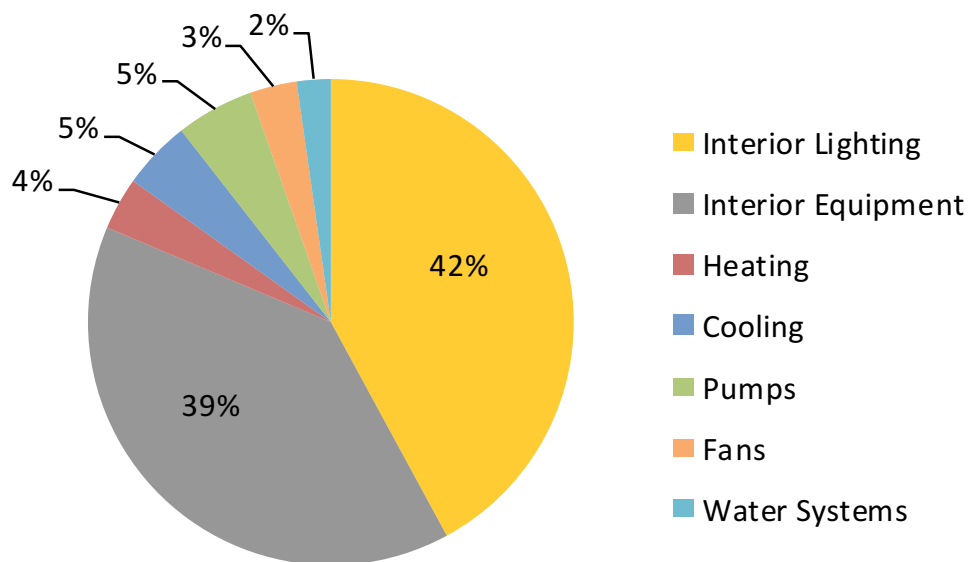
Fig. 11. Annual Energy Use Distribution in kWh/m^2

431   Fig. 12 is a psychrometric chart and shows the comfort level of all conditioned zones during occupied

432   hours at an hourly time step. The two dashed rhomboids are illustrating the comfort zones for summer

433   and winter. The control of a TABS is quite complex: Using constant supply temperatures and a

434   simplified control strategy did not allow for an effective setback during unoccupied hours.

435   Nevertheless, it was possible to control the radiant system so that the comfort levels were met almost

436   during the whole year. The very dry climate in Denver explains the low relative humidity. The slightly

437   too high relative humidity values on the top right corner of the summer comfort zone are caused by

438   the restrooms as well as the meeting rooms, whereas the outliers on the right side are only caused by

439   the closed offices.

440
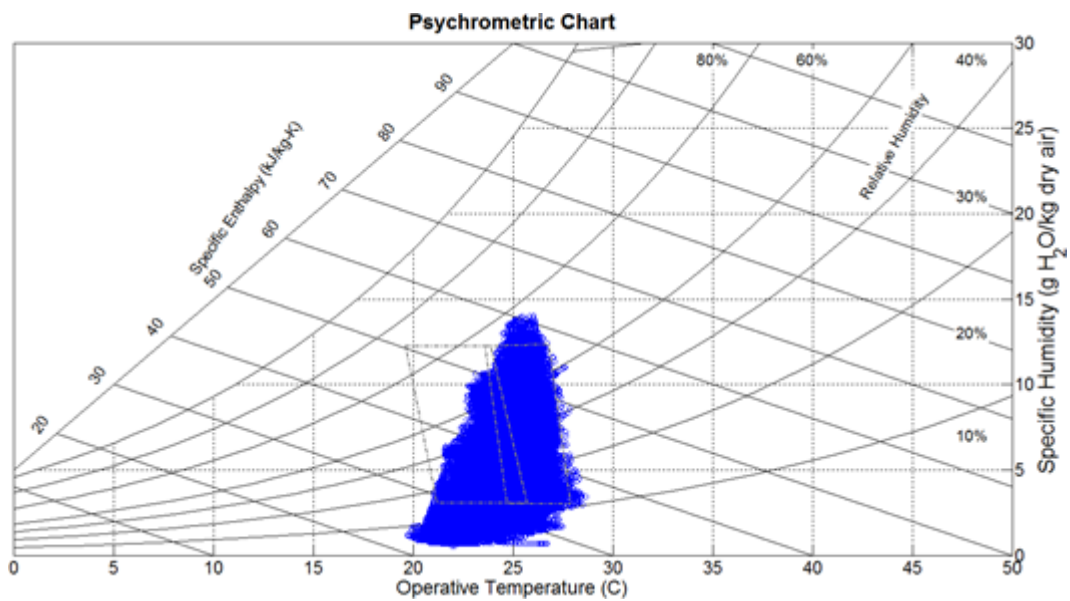
Fig. 12. Annual Comfort Chart during Occupied Hours

4.2 Reduced Order Model

Fig. 13 shows the Pareto fronts of both configurations. The Pareto front represents the trade-off among the different objective functions. These points are called non-inferior or non-dominated points (Caramia, Dell'Olmo 2008). The points on the Pareto front indicate the final optimization results whereas the dashed lines represent the exponential fit. Surprisingly, as it can be seen in Fig. 13 the combined configuration is more expensive at every reduction of ramping compared to the battery only. One reason for that may be the fairly high losses of the thermal energy storage system. Since one objective function minimizes them, the battery only configuration always performs better. According to the outcomes of this comparison, the battery only configuration was selected for further techno-economic analyses. The impact of a smaller HP in combination with a thermal storage as well as redundancy aspects have not been considered.
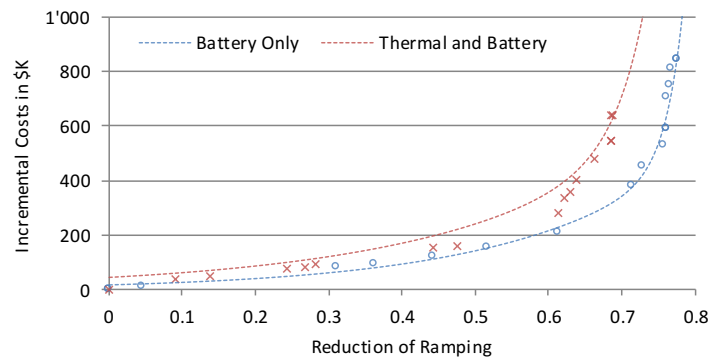
*Fig. 13. Pareto Front Costs*

The Pareto fronts in Fig. 13 clearly show that a reduction of ramping can be achieved by using a storage system. Nevertheless, such a system is only cost effective if there is an additional economic benefit for the building owner. According to current literature (Merei et al. 2016; Kosten für PV-Stromspeicher - Wirtschaftlichkeit im Detail), battery systems are not quite economical today. This statement does not include systems which are subsidized nor does it include systems where DSM is used for increasing the self-consumption rate. More detailed information about the potential value of battery storage can be found in the comprehensive report from the Rocky Mountain Institute (Rocky Mountain Institute 2015). One paper even considered retail electricity prices of 25ct/kWh and feed-in compensations as low as 2.5ct/kWh. The configuration with storage could only show its profitability when battery system

466 prices are below 200$/kWh (Merei et al. 2016). Since the impact of ramping caused by ZEB is not

467 significant yet, no literature related to the value of ramping reduction incentives could be found.

468 Therefore, the optimization problem was conducted several times with different battery system costs

469 (colored curves in Fig. 14). While utilities are currently not rewarding customers for a reduction of

470 ramping, in the future this could become an option for them when feed-in power from decentralized

471 electricity production increases rapidly. Fig. 14 shows the Pareto front family with four linear benefit

472 curves (hypothetical incentives paid by the utility). Since a ZEB with a large PV system requires a larger

473 battery system to adequately reduce ramping, the benefits depend on the PV system's peak installed

474 power. In this study, neither the electricity price nor the feed-in compensation were considered. The

475 incremental costs are investments cost.
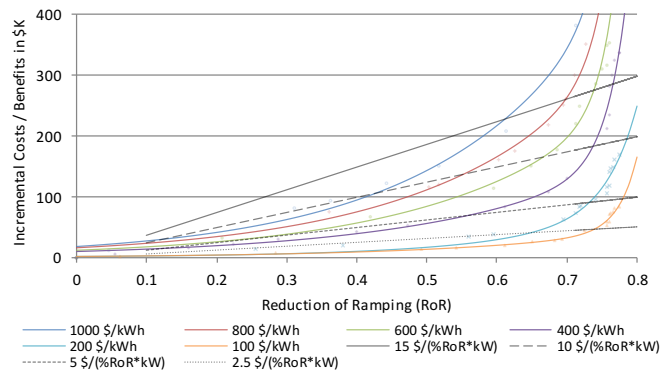

Fig. 14. Pareto Front Family Battery System

4.3   Residual Loads

479 The results from the building simulation as well as the PV system model allowed a deeper examination

480 of the changes in residual loads. Fig. 15 illustrates the annual and weekly residual loads as well as the

481 residual load duration curve. For the weekly graph, a typical week in July was considered. Due to the

482 combination of roof and façade mounted PV panels, no production drop can be noticed in winter.

483 Subtracting the PV production from the total consumption, leads to an annual PV overproduction of

484 34 MWh. Hence, the designed building is not just net zero, it is net positive.

487   Even though today it may not be economical to purchase a battery system in combination with the PV

488   system, a case study was used to show the effect on the residual loads. A capacity of 250 kWh which

489   reaches a reduction of ramping of 50 % was selected. Fig. 15 reveals the differences in residual loads

490   with and without battery storage. Because no predictive control strategy was considered and because

491   the selected battery capacity was not sufficiently large, the peak demand as well as the peak feed-in

492   power could not be lowered. Nevertheless, the hours of negative residual loads, where electricity is

493   feed into the grid could be reduced by 1948 hours. This is a very significant reduction by a factor of

494   3.6.

495
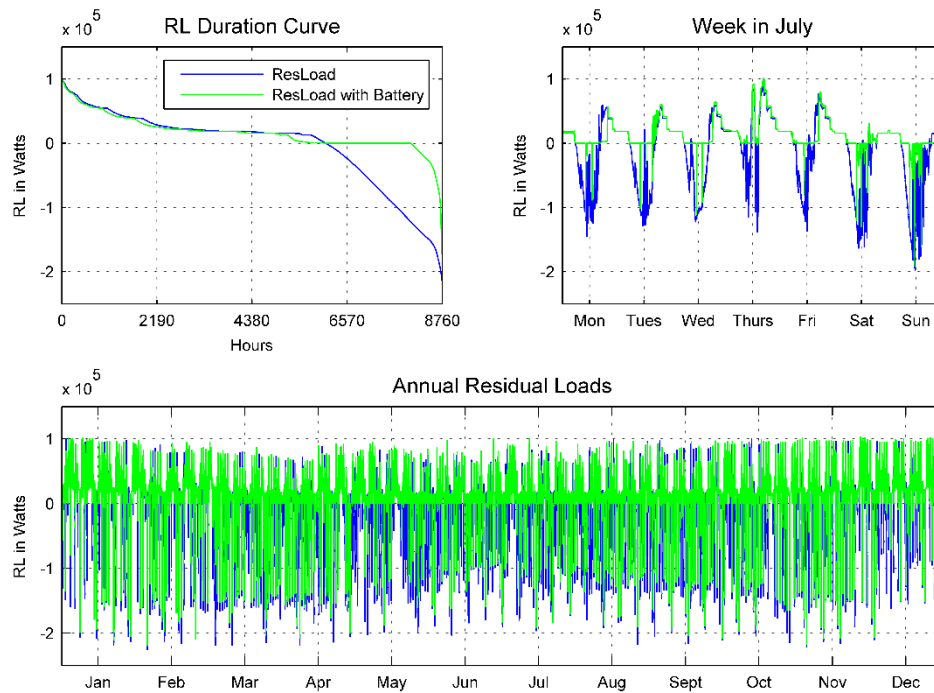
496

497   *Fig. 15. Residual Loads with Battery System (normalized)*

498

499

5. Conclusion

Though OpenStudio does not provide the same functionality as EnergyPlus yet, it was possible to design and simulate a zero energy building with an advanced HVAC system in the OpenStudio environment. Combining the building model with a photovoltaic model showed that the proposed building not only reaches net zero, it even reaches net positive status. Further analysis of residual loads as well as strategies for their reduction, showed the limited potential due to the comparatively high shares from interior lighting and equipment to the end energy use breakdown. Using a multiple objective optimization approach in combination with a simplified storage model allowed comparing different control strategies for residual load reduction. The Pareto front family illustrates which monetary incentives would be required at different battery storage prices to achieve profitability of a battery storage system.

5.1   Future Work

While the main objectives have been achieved, there are open questions and opportunities for improvements. Since the building model was quite complex, it would make sense to reduce the complexity such that the whole HVAC system could be included in the residual load reduction strategy or the entire model could be optimized. One possibility would be a reduction in the count of thermal zones or the adoption of a reduced order model. To maintain a high level of accuracy, the reduced order model could also be trained with data taken from the whole building model. At this point the storage model and its control are highly simplified; further analysis would therefore focus on a more detailed model and control. Additionally, different control strategies should be elaborated and compared. In this respect, a sensitivity analysis could help identifying the dominant factors. Residual load swings due to widespread construction of ZEB's may pose a risk for regional transmission operators (RTO) and utilities in the future, and thus, a collaboration with these entities could help identifying key risks and possible solutions for individual ZEB's or portfolios thereof.

Acknowledgements

Publication bibliography

AGFW (2015): Calculation of Thermal Losses of Thermal Energy Storages, checked on 3/28/2017.

ASHRAE (2010): Energy Standard for Buildings Except Low-Rise Residential Buildings. 90.1-2010.

ASHRAE (2014a): Advance Energy Design Guide for Small to Medium Office Buildings, checked on 5/28/2016.

ASHRAE (2014b): Advance Energy Design Guide for Small to Medium Office Buildings.

Athienitis, Andreas K.; O'Brien, William (2015): Modelling, design, and optimization of net-zero energy buildings (Solar heating and cooling).

Buchmann, Isidor (2016): What does Elevated Self-discharge do? Available online at http://batteryuniversity.com/learn/article/elevating_self_discharge, checked on 5/28/2016.

Building Component Library. Available online at https://bcl.nrel.gov/, checked on 5/28/2016.

Caramia, Massimiliano; Dell'Olmo, Paolo (2008): Multi-Objective Management in Freight Logistics. Increasing Capacity, Service Level and Safety with Optimization Algorithms. London: Springer, checked on 6/5/2016.

Çomaklı, Kemal; Yüksel, Bedri (2003): Optimum insulation thickness of external walls for energy saving. In *Applied Thermal Engineering* 23 (4), pp. 473–479. DOI: 10.1016/S1359-4311(02)00209-0.

Faktor Verlag AG - Architektur, Technik. Energie. Informationen zur Nachhaltigkeit am Bau - TABS-Tool. Available online at http://www.faktor.ch/tabs-tool.html, checked on 5/28/2016.

Fundamentals. Chapter 28 (1997), checked on 5/28/2016.

Hall, Monika (2014): Nullenergiebeäude - die nächste Generation energieeffizienter Bauten.

Henze, Gregor P. (2016): HVAC Systems: Overview. University of Colorado Boulder, 2016.

Informationsdienst, BINE: Thermoaktive Bauteilsysteme. Nichtwohnungsbauten energieeffizient heizen und kühlen auf hohem Komfortniveau, checked on 5/29/2016.

IRENA (2015): BATTERY STORAGE FOR RENEWABLES. MARKET STATUS AND TECHNOLOGY OUTLOOK. With assistance of International Renewable Energy Agency.

Jozsef Nyers, Slavica Tomic, Arpad Nyers (2014): Economic Optimum of Thermal Insulating Layer for External Wall of Brick. In *APH* 11 (7). DOI: 10.12700/APH.11.07.2014.07.13.

Judex, Florian (2012): Grid Friendly Building.

Kolokotsa, D.; Rovas, D.; Kosmatopoulos, E.; Kalaitzakis, K. (2011): A roadmap towards intelligent net zero- and positive-energy buildings. In *Solar Energy* 85 (12), pp. 3067–3084. DOI: 10.1016/j.solener.2010.09.001.

Kosten für PV-Stromspeicher - Wirtschaftlichkeit im Detail. Available online at http://www.energieheld.de/photovoltaik/stromspeicher/kosten, checked on 5/29/2016.

Martin Jakob (2004): Die optimale Dämmstärke. Wo liegt das wirtschaftliche Optimum der Wärmedämmung bei Neubauten und Gebäudeerneuerungen?, 2004, checked on 5/28/2016.

Merei, Ghada; Moshövel, Janina; Magnor, Dirk; Sauer, Dirk Uwe (2016): Optimization of self-consumption and techno-economic analysis of PV-battery systems in commercial applications. In *Applied Energy* 168, pp. 171–178. DOI: 10.1016/j.apenergy.2016.01.083.

Milo, Aitor; Gaztañaga, Haizea; Etxeberria-Otadui, Ion; Bacha, Seddik; Rodríguez, Pedro (2011): Optimal economic exploitation of hydrogen based grid-friendly zero energy buildings. In *Renewable Energy* 36 (1), pp. 197–205. DOI: 10.1016/j.renene.2010.06.021.

Nematchoua, Modeste Kameni; Raminosoa, Chrysostôme R.R.; Mamiharijaona, Ramaroson; René, Tchinda; Orosa, José A.; Elvis, Watis; Meukam, Pierre (2015): Study of the economical and optimum thermal insulation thickness for buildings in a wet and hot tropical climate: Case of Cameroon. In *Renewable and Sustainable Energy Reviews* 50, pp. 1192–1202. DOI: 10.1016/j.rser.2015.05.066.

NREL (2015): OpenStudio QuickStart Guide. Available online at https://nrel.github.io/OpenStudio-user-documentation/img/pdfs/openstudio_interface_quickstart.pdf, checked on 4/1/2017.

NSRDB (Ed.): Alphabetical List by State and City. Available online at http://rredc.nrel.gov/solar/old_data/nsrdb/1991-2005/tmy3/by_state_and_city.html, checked on 5/28/2016.

NSRDB (Ed.): Brief Summary of the TMY3. Available online at http://rredc.nrel.gov/solar/old_data/nsrdb/1991-2005/tmy3/, checked on 5/28/2016.

Rob Guglielmetti: Daylighting: Strategies, Simulation and Metrics. University of Colorado Boulder.

Rocky Mountain Institute (2015): THE ECONOMICS OF BATTERY ENERGY STORAGE. HOW MULTI-USE, CUSTOMER-SITED BATTERIES DELIVER THE MOST SERVICES AND VALUE TO CUSTOMERS AND THE GRID.

Shanti Pless: Net Zero Energy Buildings Research and Practice at NREL. NREL. University of Colorado Boulder.

Siemens: Energieeffizienz in der Gebäudeautomation, checked on 5/28/2016.

Stoffel, T.; Andreas, A. (1981): NREL Solar Radiation Research Laboratory (SRRL): Baseline Measurement System (BMS); Golden, Colorado (Data).

System Advisor Model (SAM) | (2016). Available online at https://sam.nrel.gov/, updated on 6/5/2016, checked on 6/5/2016.

U.S. Department of Energy: A Common Definition for Zero Energy Buildings, checked on 5/27/2016.

U.S. Department of Energy (Ed.): Ductless Mini-Split Air Conditioners | Department of Energy. Available online at http://energy.gov/energysaver/ductless-mini-split-air-conditioners, checked on 5/29/2016.

U.S. Department of Energy: The Design-Build Process for the Research Support Facility (RSF), checked on 5/28/2016.

U.S. Department of Energy (2015): Quadrennial Technology Review - An Assessment of Energy Technologies and Research Opportunities, pp. 11–32, checked on 5/26/2016.

U.S. Department of Energy; University of California; University of Illinois: Weather Data by Location. Denver Intl AP 725650 (TMY3). Available online at https://energyplus.net/weather-location/north_and_central_america_wmo_region_4/USA/CO/USA_CO_Denver.Intl.AP.725650_TMY3, checked on 4/2/2017.

U.S. Department of Energy; University of Illinois; University of California (2015): Engineering Reference. The Reference to EnergyPlus Calculations.

UW Berg: Berg Publications. Available online at http://www.uwberg.org/publications/, checked on 4/3/2017.

609   Vogelsanger, Peter; Haberl, Robert; Frank, Elimar; Brunold, Stefan (2008): Dimensionierung solarer
610   Kombisysteme. SPF Institut für Solartechnik. 18. OTTI Symposium Thermische Solarenergie.

611   Zhu, Dandan; Hong, Tianzhen; Yan, Da; Wang, Chuang (2012): Comparison of Building Energy
612   Modeling Programs: Building Loads. Tsinghua University, China; Environmental Energy Technologies
613   Division.

614

615

616 Tables

617

618 *Table 1: Standard Percentage Assumptions by Space Type*

Space Type	Percentage of Floor Area (Guideline)	Floor Area in m^2 (Applied)	Percentage of Floor Area (Applied)
Open Office	15 %	1'397.0	17 %
Private Office	29 %	2'370.0	28 %
Conference / Meeting Room	8 %	698.0	8 %
Corridor	12 %	1'161.0	14 %
Active Storage Area	14 %	1'254.0	15 %
Restroom	4 %	312.0	4 %
Lounge	2 %	220.5	3 %
Electrical / Mechanical Room	2 %	162.0	2 %
Stairway	3 %	336.0	4 %
Lobby	6 %	350.0	4 %
Others	5 %	94.5	1 %
Total	100 %	8'355.0	100 %

619

620 *Table 2: Associated measures for daylight and energy saving optimization*

Option	Measure
1	Illuminance Sensors
2	Illuminance Sensors, Daylight redirection
3	Illuminance Sensors, Daylight redirection, interior shades
4	Illuminance Sensors, Daylight redirection, interior blinds
5	Illuminance Sensors, Daylight redirection, interior blinds, higher reflective wall and ceiling
6	Illuminance Sensors, Daylight redirection, interior blinds, higher reflective wall and ceiling, exterior shading triangle 80cm
7	Illuminance Sensors, Daylight redirection, interior blinds, higher reflective wall and ceiling, exterior shading triangle 50cm
8	Illuminance Sensors, Daylight redirection, interior blinds, higher reflective wall and ceiling, exterior shading triangle 30cm
9	Illuminance Sensors, Daylight redirection, interior blinds, higher reflective wall and ceiling, exterior shading cube 80cm
10	Illuminance Sensors, Daylight redirection, interior blinds, higher reflective wall and ceiling, exterior shading cube 50cm
11	Illuminance Sensors, Daylight redirection, interior blinds, higher reflective wall and ceiling, exterior shading cube 30cm

621

622 *Table 3: PV System Characteristics*

PV System	Capacity	Energy Production
Roof	200.0 kW	296'811 kWh
South Façade	52.6 kW	56'986 kWh
East Façade	29.5 kW	27'603 kWh
West Façade	29.5 kW	22'248 kWh

623

624

625

626 *Table 4: Annual Building Performance Key Values*

Building Performance	Site Energy	Normalized Site Energy
Total Site Energy	373'292 kWh	44.68 kWh/m^2
Total Source Energy	1'175'869 kWh	141.50 kWh/ m^2
Total EUI	-	44.68 kWh/ m^2
Interior Lighting	157'081 kWh	18.80 kWh/ m^2
Interior Equipment	146'628 kWh	17.55 kWh/ m^2
Heating	13'069 kWh	1.56 kWh/ m^2
Cooling	17'114 kWh	2.05 kWh/ m^2
Pumps	19'336 kWh	2.31 kWh/ m^2
Fans	11'642 kWh	1.39 kWh/ m^2
Service Hot Water	8'419 kWh	1.01 kWh/ m^2
EUI Conditioning	-	7.32 kWh/ m^2

627

628

List of Figures